A Chinese case of CHST3-related skeletal dysplasia and a systematic review

Hanting Liang
Peking Union Medical College Hospital
Wenting Qi
Peking Union Medical College Hospital
Chenxi Jin
Tsinghua University Affiliated Beijing Tsinghua Changgung Hospital: Beijing Tsinghua Changgung Hospital
Qianqian Pang
Peking Union Medical College Hospital
Lijia Cui
Peking Union Medical College Hospital
Yan Jiang
Peking Union Medical College Hospital
Ou Wang
Peking Union Medical College Hospital
Mei Li
Peking Union Medical College Hospital
Xiaoping Xing
Peking Union Medical College Hospital
Wei Liu
Peking Union Medical College Hospital
Weibo Xia (xiaweibo8301@163.com)
Peking Union Medical College Hospital https://orcid.org/0000-0001-7768-5536

Research Article

Keywords: Spondyloepiphyseal dysplasia with congenital joint dislocations, CHST3, vBMD, bone microarchitecture, HR-pQCT

Posted Date: October 28th, 2022

DOI: https://doi.org/10.21203/rs.3.rs-2164454/v1

Version of Record: A version of this preprint was published at Endocrine on February 2nd, 2023. See the published version at https://doi.org/10.1007/s12020-023-03303-z.

Abstract

Purpose

This study described a case with carbohydrate sulfotransferase 3 (CHST3) spondyloepiphyseal dysplasia and summarized all previously reported cases with CHST3-related skeletal dysplasia.

Methods

A 14.8-year-old boy underwent clinical and radiological evaluations, including high-resolution peripheral quantitative computed tomography. The patient and the family members underwent genetic tests. All CHST3-related skeletal dysplasia cases from PubMed and Embase were collected and analysed.

Results

The proband was found to have short lower limbs during a prenatal examination. At 11 years old, he had a compression fracture of L2. Since 13 years of age, he has complained of aggravated pain in the large joints. Physical examination showed a height Z score of -4.94, short limbs, and restricted movement of the elbows and knees. X-rays showed epiphyseal dysplasia of the carpal bones, enlargement of the left elbow and knee joints, and subluxation of the left hip. Echocardiography showed abnormal cardiac valves. Compared with the norm, his total and trabecular volumetric bone mineral density (vBMD) were significantly lower, and the microarchitecture of the trabecular bone was poor at the distal radius and tibia. Two novel missense variants of c.1343T > G and c.761C > G in *CHST3* were inherited from his father and mother, respectively. In the systematic review, short stature, limited joint extension, joint pain, and joint dislocation were the most common characteristics associated with mutations of *CHST3*. Over 90% of pathogenic variants are located in the sulfotransferase domain.

Conclusion

This patient with CHST3-related skeletal dysplasia has progressive joint pain and movement restriction, poor vBMD, and abnormalities of the microarchitecture of the trabecular bone. There is no apparent genotype-phenotype correlation in this disorder.

Introduction

Spondyloepiphyseal dysplasia (SED) with congenital joint dislocations (MIM 143095), also called “spondyloepiphyseal dysplasia, Omani type (SEDO)” or “carbohydrate sulfotransferase 3 (CHST3)-related skeletal dysplasia”, is a kind of sulfation disorder [1, 2]. It was first reported in 1974 [3], and in 2004, *CHST3* was identified as its pathogenic gene [4]. CHST3-related skeletal dysplasia is an extraordinarily rare skeletal disorder without a known incidence or prevalence, but in 2020, Duz et al. reported that there

were nearly 50 patients with CHST3-related skeletal dysplasia that had been reported worldwide [5]. CHST3-related skeletal dysplasia is mainly characterized by prenatal short stature, linear growth retardation, joint dislocation or subluxation, movement restriction of large joints, and skeletal deformities, including kyphosis, scoliosis, slight shortening of the trunk, and genu valgum [2]. Partially affected individuals have cardiac valve dysplasia and hearing impairment [5].

CHST3-related skeletal dysplasia is inherited as an autosomal recessive disorder, which means that both homozygous and compound heterozygous variants in the *CHST3* gene can result in the condition [2]. The *CHST3* gene is located at chromosome 10q22.1 and it has 3 exons; it is also sometimes called chondroitin 6-sulfotransferase 1 (C6ST-1) [6]. The CHST3 enzyme consists of 479 amino acids, which can transfer sulfate from 3'-phosphoadenosine-5'-phosphosulfate (PAPS) to position 6 of the N-acetyl galactosamine (GalNAc) residue of chondroitin sulfate [4]. The sulfation of chondroitin is crucial for maintaining the development, structure, and function of cartilage and endochondral bone [7]. Several studies have verified that biallelic variants of the *CHST3* gene lead to loss of function of the CHST3 enzyme and a sharp reduction of CHST3 enzyme activity, to the point its activity can hardly be detected in urine or fibroblasts collected from patients [4, 8, 9].

This study reported a SED case with two novel *CHST3* compound heterozygous variants, evaluated the affected individual's volumetric bone mineral density (vBMD) and bone microarchitecture by high-resolution peripheral quantitative computed tomography (HR-pQCT), and summarized the clinical, radiological, and genetic characteristics of all known affected cases with *CHST3* biallelic variants by a systematic review.

Materials And Methods

Subjects

A 14.8-year-old boy was referred to our department due to progressive joint pain for two years. The birth history, clinical manifestations, family information, and physical examination of the affected individual were recorded in detail. Peripheral blood samples of the affected patient, his parents, and his older sister were collected for genetic tests. The patient and the family members signed informed consent forms for the genetic tests. This study was performed with the approval of the Ethics Committee of Peking Union Medical College Hospital (JS-1689) and following the Declaration of Helsinki.

Biochemical assays

Fasting blood samples and urine samples were collected to detect biochemical parameters. The blood and urine routine tests, liver function, renal function, serum calcium, serum phosphorus, alkaline phosphatase (ALP), bone turnover markers, including β-C-terminal telopeptide (β-CTX), antinuclear antibody spectrum, and autoantibodies of rheumatoid arthritis and human leucocyte antigen-B27 (HLA-B27) were measured by an autoanalyzer. Hormones of anterior pituitary axes, including growth hormone (GH), insulin-like growth factor-1 (IGF-1), thyroid function, adrenocorticotropic hormone, cortisol, sex

hormones, total 25-hydroxy vitamin D (T25OHD) and parathyroid hormone (PTH), were detected by the chemiluminescence method. All of these parameters were measured, and the reference ranges were obtained from the Department of Clinical Laboratory of Peking Union Medical College Hospital.

HR-pQCT evaluation

An HR-pQCT scan (XtremeCT II scanner, ScancoMedical, Brüttisellen, Switzerland) was performed on the nondominant distal radius and distal tibia of the patient and 5 age-matched healthy boys. The protocol was described previously [10–13]. In brief, all of them were asked to keep their distal forearm and distal leg immobilized in a carbon fibre cast and remain silent for at least 2 minutes and then scanned according to a protocol (voltage 68 kVp, current 1.47 mA, integration time 43 ms, matrix size 2304 × 2304) previously described for obtaining bone geometry, vBMD and microarchitecture parameters. When a qualified scan was finished, the reference line was placed at the distal endplate of the nondominant radius and tibia. A stack of 168 CT slices was acquired 9.0 and 22.0 mm proximal to the reference line for the distal radius and tibia, respectively. Images were acquired with an isotropic resolution of 61 μm. The Image Processing Language (v5.42, Scanco Medical) algorithm was used for the identification of the endosteal surface and segmentation of the cortical and trabecular compartments. After successful compartment segmentation, the total area (Tot.Ar), trabecular area (Tb.Ar), cortical area (Ct.Ar), total vBMD (Tot.vBMD), trabecular vBMD (Tb.vBMD), cortical vBMD (Ct.vBMD) and perimeter (Ct.Pm) were directly measured. Parameters of bone microarchitecture were calculated directly, including trabecular thickness (Tb.Th), separation (Tb. Sp), number (Tb.N), bone volume fraction (Tb.BV/TV), inhomogeneity of network (Tb.1/N.SD), cortical porosity (Ct.Po), thickness (Ct.Th) and cortical pore diameter (Ct.Po.Dm).

Genetic testing by whole-exome sequencing (WES)

Genomic DNA (gDNA) of the patient and family members was extracted from peripheral blood by the QIAamp DNA Mini Kit (51304, QIAGEN, Germany). As a standard procedure, WES was performed on the gDNA of the patient. In brief, the gDNA was broken into 100 ~ 500 bp fragments by a BGI enzyme kit (Segmentase, BGI), and then 280 ~ 320 bp fragments were selected with magnetic beads. After repairing the ends, the collection added an “A” base at the 3’ overhangs. Then, a single individual DNA library was built after LM-PCR and purification. The library was enriched by array hybridization (Roche NimbleGen, USA), followed by elution and postcapture amplification. The qualified products were pooled, quantified, and sequenced on MGISEQ-2000. Raw data of the sequencing reads were filtered and aligned to a reference human genome (hg19) using Burrows–Wheeler Aligner software, and single-nucleotide variants, insertions and deletions were detected using Genome Analysis Toolkit 4.0 (Broad Institute) software, followed by alignment of the database (NCBI dbSNP, HapMap, the 1000 Genomes dataset and a database of 100 healthy Chinese adults) to be screened for suspicious variants.

Verification of CHST3 variants by Sanger sequencing

For further verification, the gDNA of the patient and the family members was amplified by polymerase chain reaction (PCR) to detect *CHST3* (NM 004273.5) variants. The amplification system included 10 μl

of 2×Dream Taq PCR Master Mix (Thermo Fisher Scientific, USA), 6 μl of double-distilled water, 2 μl of genomic DNA, and 1 μl of forward and reverse primers. The forward and reverse primers for c.761C > G were 5′-ACTCAGTTCATGTTCCGCCG-3′ and 5′-TCTTCTGCGTGGAGTAGATGC-3′, and those for c.1343T > G were 5′-AGAAGGCCCGCGAGATGTA-3′ and 5′-CTTTCACGAGGAGGGGCATAC-3′. The PCR cycling conditions were one cycle at 94°C for 4 minutes; 35 cycles at 94°C for 30 seconds, appropriate annealing temperatures for 30 seconds and 72°C for 30 seconds; and one cycle at 72°C for 4 minutes followed by storage at 4°C. Sanger sequencing was performed for variant detection. The pathogenicity of two *CHST3* variants was graded according to the American College of Medical Genetics and Genomics (ACMG) guidelines [14].

Systematic review

Searching the PubMed and Embase databases based on the items of "(CHST3) AND (mutation)" or "(CHST3) AND (spondyloepiphyseal dysplasia)", a total of 19 English-language studies of CHST3-related skeletal dysplasia (up to December 31st, 2021) were included [5, 6, 8, 9, 15–29]. All available data were extracted for further analysis, mainly including clinical, radiological, and genetic information.

Statistical analysis

All available data were analysed by using SPSS version 25.0. Data following a normal distribution are displayed as the mean ± standard deviation, and data with an abnormal distribution are depicted as the median (interquartile range, IQR). For parameters evaluated by HR-pQCT, the normally distributed data of the patient and the control group were compared by the one-sample t-test, and the abnormally distributed data were compared by the Wilcoxon signed-rank test. Z scores of heights between different groups were compared by independent-sample t-tests. Bivariate analysis was applied to determine the relationship between two parameters. Fisher's exact test was performed between two groups with categorical data. A p value less than 0.05 indicated a statistically significant difference.

Results

Clinical case

The 14.8-year-old affected boy was the second child of the parents, born vaginally at full term, with a birth weight of 2.95 kg and an unknown birth length. Prenatal examination by ultrasound indicated that the lower limbs were short. The developmental milestones were similar to those of peers. Since 6 years old, he had difficulty squatting down and was shorter in stature than his peers. Meanwhile, chest pain occasionally occurred. At 7.8 years old, he went to the local hospital due to short stature with a height of 108.4 cm (Z score: -3.93). Further evaluation showed that the peak value of GH was 11.51 ng/ml by a GH stimulation test, the level of IGF-1 was 160 ng/ml (reference range, RR: 64 ~ 345 ng/ml), the second lumbar vertebrae (L2) was relatively small and the spine was kyphotic by X-ray, no pathogenic variant was found in the fibroblast growth factor receptor 3 gene by Sanger sequencing, and the levels of enzymes related to mucopolysaccharidosis were all within the normal ranges. Therefore, he was

diagnosed with “idiopathic short stature” and accepted recombinant-human growth hormone (rhGH) therapy with a dosage of 0.15 IU/kg for 3 years. His height Z score increased from − 3.93 to -3.0.

At 11 years old, he experienced sudden low back pain one morning, and he was diagnosed with a “compression fracture of L2”. After accepting conservative management, the condition improved. Since approximately 13 years old, he complained of aggravated bone and joint pain, most obviously in the shoulders, waist, hip, knees, and lower limbs. However, there was no obvious pain in his wrists and ankles. Daily activities, such as walking, were influenced by genu valgum. His intelligence was normal. Puberty had not started yet. The growth chart and time points of pain starting at different sites are shown in Fig. 1. His family members were all healthy. The heights of his father and mother were 172 cm and 157 cm, respectively, and it was a nonconsanguineous marriage. His older sister was 22 years old, with a height of 167 cm.

Physical examination at 14.8 years old showed a height of 139.2 cm (Z score: -4.94), a weight of 45 kg, and a head circumference of 55.5 cm (Fig. 2.A ~ B). There was a grade soft blowing-like systolic murmur between the second intercostal at the left edge of the sternum. He had a short neck, short limbs, restricted movement and contractures of the elbows and knees, and no obvious hyperextension of the metacarpophalangeal joints. His visual analogue score of tenderness from the thoracic to lumbar spinous process reached 6 ~ 7 points, and it reached 8 points for thorax compression pain. The right lower limb was slightly longer than the left lower limb, and while standing naturally, the distances between the two tibias and two ankles were 3.5 cm and 17 cm, respectively. The vision and audition were normal.

The results of the biochemical tests were as follows: T25OHD was 18.3 ng/ml. The antinuclear antibody spectrum, autoantibodies of rheumatoid arthritis, and HLA-B27 were all negative. Other parameters, including hormones of the anterior pituitary axes, calcium, phosphorus, ALP, β-CTX, and PTH, were all within the normal ranges. Spine X-ray indicated small vertebrae of L2 at 1 year old (Fig. 2.C ~ D) and thoracic kyphosis, lumbar lordosis, sacral kyphosis, and compression fracture of L2 at 14.8 years old (Fig. 2.E). Three-dimensional computed tomography of the spine displayed compression fracture of L2, scoliosis, and changes in the physiological curve of the spine at 12 years old (Fig. 2.F). Moreover, X-rays also showed epiphyseal dysplasia of the carpal bones (Fig. 2.G), enlargement of the left elbow joint and knee joints (Fig. 2.H ~ I), flat acetabulum, shortening of the femoral neck, subluxation of the left hip, and deformities and arthritis of the sacroiliac and hip joints (Fig. 2.J). Echocardiography indicated mild aortic valve stenosis with insufficiency and a suspected bicuspid aortic valve.

Therefore, the patient was diagnosed with “spondyloepiphyseal dysplasia” clinically.

Parameters evaluated by HR-pQCT

Data on bone geometry, vBMD, and bone microarchitecture of the radius and tibia in the control group and the affected individual are shown in Table 1. Both at the radius and the tibia, Ct.Ar in the patient was significantly lower than that in the control group. At both the radius and tibia, Tot.vBMD and Tb.vBMD in

the patient were significantly inferior to those in the control group. However, the Ct.vBMD of the patient was slightly lower than that of the mean value in the control group at these two sites, without significant differences. For bone microarchitecture, values of Tb.BV/TV and Tb.Th in the patient were significantly lower than those in the control group at the radius and tibia. In addition, compared with the control group, Ct.Th at the tibia and Ct.Po.Dm at the radius of the patient were significantly decreased. Representative three-dimensional images of the radius and tibia from the affected individual and a 15-year-old healthy boy are shown in Fig. 3.

Genetic results of the proband and family members

Two novel heterozygous variants of the *CHST3* gene were identified in the proband by WES, including c.1343T > G (p.M448R) and c.761C > G (p.P254R). Further Sanger sequencing confirmed that the c.1343T > G variant was inherited from the father and the c.761C > G variant was inherited from the mother. Neither variant was detected in the older sister. The pedigree and the results of Sanger sequencing are shown in Fig. 1 of the supplementary materials. According to the ACMG guidelines, these two novel variants were judged as likely pathogenic variants (Supplementary Table 1). According to the typical characteristics and the clear genetic testing result, the proband was diagnosed with spondyloepiphyseal dysplasia with congenital joint dislocations.

Systematic review

As of December 31st, 2021, a total of 77 affected patients had been reported among 46 families, of whom 70 individuals had a clear genetic diagnosis, including the affected individual in this study and two aborted fetuses. A family history of short stature accounted for 37.5% (9/24). The proportions of consanguineous marriage, suspected endogamous marriage, and nonconsanguineous marriage accounted for 59.3% (16/27), 11.1% (3/27), and 29.6% (8/27), respectively. The median age of diagnosis was 10 years old (IQR: 5.8 ~ 17.0 years old). A total of 69.6% (32/46) of patients were found to have short limbs during the prenatal examination or joint dislocation after birth. The birth length was 37 ~ 46 cm of 27 affected individuals, and the birth weight was 2.1 ~ 3.5 kg of 7 affected individuals.

The mean Z score of heights was − 4.86 ± 1.48 (n = 30). The height Z scores of males and females were comparable, -4.71 ± 1.59 (n = 20) vs. -5.28 ± 1.25 (n = 9), p = 0.335 (Fig. 4.A). The Z score of heights in the children was significantly higher than that in the adults, with the mean values of -4.57 ± 1.40 (n = 24) for the children and − 6.01 ± 1.30 (n = 6) for the adults, p = 0.030 (Fig. 4.B). Further bivariate analysis indicated that the age at evaluation and the height Z scores had a negative correlation (r=-0.55, p = 0.003, n = 27, Spearman analysis, Fig. 4.C). The proportions of clinical and radiological characteristics are summarized in Table 2. Short stature, limited joint extension, joint pain, waddling gait, joint dislocation or subluxation, and rhizomelic shortening were the most common clinical manifestations. Approximately 98% of patients had normal intelligence. Hearing impairment was found among 42.9% of patients. As far as we know, apart from our case, no study has reported fractures in affected individuals with CHST3-related skeletal dysplasia. An abnormal vertebral shape, epiphyseal dysplasia, shortening of the femoral neck, joint enlargement, and osteoarthritis were the most common X-ray changes. Cardiac involvement

accounted for 84% by echocardiography, mainly affecting the structure and function of the valves, in which mitral/tricuspid regurgitation and aortic/pulmonary valve stenosis were most common, but ventricular septal defect and valve thickening were relatively less common.

Therapeutic data are limited. Only two patients had accepted rhGH therapy, including the patient in this study. The other patient was treated with rhGH for three years but did not acquire the ideal efficacy. Moreover, that patient developed scoliosis. Seven patients accepted orthopaedic surgeries many times. In addition, one patient accepted the atlantoaxial fixation surgery due to atlantoaxial instability.

Among 70 patients with pathogenic variants of *CHST3*, 81.4% had homozygous variants, and 18.6% had compound heterozygous variants. A total of 44 pathogenic *CHST3* variants are shown in Fig. 4.D and Table 2 of the supplementary materials. Variants of missense, nonsense, and frameshift accounted for 63.6%, 22.7%, and 6.8%, respectively. Deletion and insertion, fragment deletion, and splicing variants all accounted for 2.3%. A total of 95.5% of the variants were located in exon 3, and 90.9% of the variants were located in the sulfotransferase domain.

Then, we explored whether there was a correlation between the genotype and the phenotype of this condition. Height Z score and hearing were chosen as the representative characteristics of the phenotype. *CHST3* variants were classified into a missense variant group and a nonmissense variant group, and the latter group included nonsense and frameshift variants. Height Z scores between the two groups were comparable, with mean values of -4.82 ± 1.42 (n = 14) in the missense group and − 4.48 ± 1.39 (n = 12) in the nonmissense group (p = 0.533). There were 66.7% (6/9) patients with normal hearing in the missense group and 45.5% (5/11) patients with normal hearing in the nonmissense group (p = 0.406, Fisher's exact test).

Discussion

The 2019 version of the nosology and classification of genetic skeletal disorders includes 461 disorders divided into 42 groups involving 437 pathogenic genes [1]. Among these genes, the related pathogenic mechanisms mainly involve abnormalities in the extracellular matrix (ECM), signalling pathways, transcription factors, enzymes, channel proteins, mineralization processes, and so on [30]. CHST3-related skeletal dysplasia is a type of SED due to a sulfation disorder [30], with no more than 80 cases reported worldwide until 31 December 2021 according to our count. Indeed, variants in the *CHST3* gene reduce its enzyme activity sharply [4, 8], but it seems not to affect the expression of the CHST3 enzyme, at least in the variant of p.T141M [26]. Since proteoglycans (PGs) consist of a core protein attached to one to over one hundred glycosaminoglycans (GAGs), the normal sulfation process in GAGs is fundamental for PGs playing their roles in the cellular nucleus, cytoplasm, and ECM [30, 31]. However, whether CHST3 variants change the downstream signalling pathways of chondrocytes, osteoblasts and osteoclasts remains unknown.

Similar to the results of the systematic review in this study, other studies demonstrated that prenatal and postnatal growth retardation, congenital joint dislocation, movement restriction of large joints, and

skeletal deformities, including kyphosis, scoliosis, genu valgum, and clubfeet, are the most typical clinical manifestations of patients with CHST3-related skeletal dysplasia [2, 5]. Even if the clinical characteristics mentioned above are well known, the following manifestations still deserve attention: joint pain, short stature, hearing impairment, and cardiac involvement. First, among 4 patients with joint pain and a record of the onset age, joint pain often appears around the age of ten and mainly involves the hip and knee joints [26, 27]. Similar to osteoarthritis and Kashin-Beck disease, chondrocytes in these two disorders lack CHST3 expression [32, 33]. Second, it is inferred that the negative correlation between height Z scores and age at evaluation may be the comprehensive result of aggravation of spinal deformities, flattening of the intervertebral discs, growth retardation of long bones, and aggravation of the lower limb deformities. In 2013, Song et al. showed that CHST3 was a susceptibility gene for lumbar disc degeneration [34], which might provide partial evidence for the conjecture above. Third, there are approximately 43% of patients have conductive hearing impairment, which may result from ossicular malformation in the middle ear [5]. Finally, CHST3 is highly expressed in the heart [35], so CHST3 deficiency may cause mild abnormalities in cardiac structure, especially the cardiac valves. However, not all reported patients were evaluated with echocardiograms or accepted cardiac function assessment.

In this study, we evaluated the vBMD and bone microarchitecture of a patient with CHST3-skeletal dysplasia for the first time. Tot.vBMD, Tb.vBMD, Tb. BV/TV and Tb.Th in the patient were inferior to those in the control group at the distal radius and tibia, and he had a history of L2 compression fracture, which might be related to the small size and congenital weakness of this vertebrae, indicating that we should pay attention to the BMD and the fracture risk of these patients.

As Fig. 3 shows, the microarchitecture of the trabecular bone at the distal tibia in the patient was poor relative to the controls. For the cortical bones, Ct.Th of the patient was lower than that of the controls at the distal tibia, but it was comparable at the distal radius between the patient and the controls. This phenomenon may be explained by Wolff's law; that is, mechanical loading remodels bones by strengthening the spongy and cortical bones [36], while the mechanical loading in the lower extremities of the patient was not as heavy as that in the controls due to joint pain, movement restriction and decreased activity capacity. The mechanism by which *CHST3* variants change the vBMD and bone microarchitecture remains unknown. It is cautiously inferred that incomplete sulfation of chondroitin sulfate influences the components and function of the ECM.

The following clinical characteristics may help with the diagnosis of CHST3-related skeletal dysplasia, including short limbs during the prenatal examination, congenital joint dislocation, and osteoarthritis since the first decade. Due to the prominent clinical and radiological features, it is not difficult to make a clinical diagnosis of SED, but a definite diagnosis still relies on genetic tests. CHST3-related skeletal dysplasia should be differentiated from other types of SED. Table 3 summarizes the key points for differential diagnosis in common types of SED. SED congenital (SEDC) is caused by pathogenic variants in the collagen type II alpha 1 chain (*COL2A1*) gene, characterized by severe disproportionate short stature after birth, prominent facial features, ophthalmological complications, and hearing loss [37], but these characteristics are not common in CHST3-related skeletal dysplasia. Osteoarthritis, joint stiffness,

and progressive joint pain involving almost all large and small joints are the typical characteristics in spondyloepiphyseal dysplasia tarda with progressive arthropathy (SEDT-PA), which results from Wnt-inducible signalling pathway protein 3 (*WISP3*) gene variants [38]. The onset age of the disorder is between 3 ~ 8 years old, but the diagnosis is often only made in the second decade, and anti-inflammatory therapy is not effective [38]. Spondyloepiphyseal dysplasia tarda (SEDT) is a X-linked recessive disorder and caused by transport protein particle complex 2 (TRAPPC2) gene mutations, mainly manifesting as progressive osteoarthritis of large joints onset during 5 ~ 10 years old [39].

To date, a total of 44 pathogenic variants in *CHST3* have been reported, including two novel variants in our study. The percentage of missense variants is the highest, reaching nearly 64%. Similar to previous studies, we did not find genotype-phenotype correlations [5, 25]. This may be because over 90% of variants are located in the sulfotransferase domain, and all loss-of-function variants reduce the enzyme activity, so the phenotype is homogeneous among patients with CHST3-related skeletal dysplasia [2, 4].

Regardless of the severity of the disorder, there are no effective methods for treatment. The treatment experience with rhGH is limited, but rhGH is not recommended for these patients due to poor efficacy and its aggravation of scoliosis [8]. The height Z score of our patient had improved by approximately 1 standard deviation after rhGH therapy, but he was still short of stature. Most patients accept orthopaedic surgeries many times to ameliorate their activity abilities [6, 9, 17, 22, 24]. Whether anodyne can help relieve joint pain effectively in these patients is not clear. During follow-up, in addition to activity, joint function, and joint pain, the extraskeletal manifestations deserve attention and evaluation, including hearing examinations and echocardiograms. The prognosis and clinical outcome have not been reported previously, but it is important to pay attention to the psychological condition, quality of life, pain management, and longevity of these patients.

The strengths of this study are as follows: (1) the identification of two novel variants in *CHST3* expands the mutation spectrum of the gene; (2) to the best of our knowledge, this study evaluates the bone geometry, vBMD, and bone microarchitecture in patients with CHST3-related skeletal dysplasia for the first time by HR-pQCT; and (3) the clinical, radiological and genetic characteristics of the disorder are reviewed and summarized comprehensively, and the genotype-phenotype correlations are also explored preliminarily.

There are also limitations in this study. First, functional studies were not performed to verify a damaging effect of the two novel variants in the *CHST3* gene, such as detection of the enzyme activity. Second, the results evaluated by HR-pQCT of the affected individual in this study cannot represent the bone health condition of all patients with CHST3-related skeletal dysplasia. Although GH is a strong anabolic agent influencing skeletal growth, the influence of rhGH on the vBMD and bone microarchitecture of this patient remained unclear, since there was a four-year interval between the cessation of rhGH therapy and the evaluation of HR-pQCT. Finally, to a certain extent, the results of the systematic review may have a bias due to the limited data extracted from the literature.

In conclusion, this study reported a CHST3-related skeletal dysplasia case with two novel *CHST3* compound heterozygous variants. The affected individual had lower total and trabecular vBMD than their peers and a history of compression fracture of L2, so they should be made aware of their increased fracture risk. By systematic review, short stature, limited joint extension, joint pain, and joint dislocation are the typical characteristics of this disorder, and height Z scores and age at evaluation have a negative correlation. Moreover, missense variants are the most common type in the *CHST3* gene. There is no genotype-phenotype correlation in CHST3-related skeletal dysplasia.

Declarations

Conflict of interest

All authors declare that they have no conflict of interest.

Data availability statement

The raw datasets generated and/or analyzed during this study are not publicly available but are available from the corresponding author on reasonable request.

Funding

This study was supported by the National Natural Science Foundation of China (81970757), the Chinese National Key Technology R & D Program, Ministry of Science and Technology (2021YFC2501700), and the Chinese Academy of Medical Sciences-CAMS Innovation Fund for Medical Sciences (CIFMS-2021–12M-1–002).

Author contributions

WB Xia and Wei L designed the study and revised the manuscript. QQ Pang collected the blood samples. HT Liang analyzed the genetic results. HT Liang analyzed all data and draft the manuscript. WT Qi and CX Jin collected HR-pQCT data. LJ Cui, W Liu, Y Jiang, O Wang, M Li, XP Xing and WB Xia collected clinical information of patients. HT Liang and WB Xia are responsible for the integrity of the data analysis. All authors read and approved the final manuscript.

Ethics approval

The study was performed with the approval of the Ethics Committee of Peking Union Medical College Hospital (JS-1689).

Consent to participate

All of the subjects agreed to participate in this study and signed informed consent forms.

Acknowledgement

We greatly appreciate to all of the participants in this study. This study was supported by the National Natural Science Foundation of China (81970757), the Chinese National Key Technology R & D Program, Ministry of Science and Technology (2021YFC2501700), and the Chinese Academy of Medical Sciences-CAMS Innovation Fund for Medical Sciences (CIFMS-2021–12M-1–002).

References

1. Mortier GR, Cohn DH, Cormier-Daire V, Hall C, Krakow D, Mundlos S, et al. Nosology and classification of genetic skeletal disorders: 2019 revision. American journal of medical genetics. Part A 179:2393-2419 (2019)
2. Superti-Furga A, Unger S. CHST3-Related Skeletal Dysplasia. In: Adam MP, Ardinger HH, Pagon RA, Wallace SE, Bean LJH, Gripp KW, Mirzaa GM, Amemiya A (eds) GeneReviews(®). University of Washington, Seattle Copyright © 1993-2021, University of Washington, Seattle. GeneReviews is a registered trademark of the University of Washington, Seattle. All rights reserved., Seattle (WA)(1993)
3. Kozlowski KS, Celermajer JM, Tink AR. Humero-spinal dysostosis with congenital heart disease. American journal of diseases of children (1960) 127:407-410 (1974)
4. Thiele H, Sakano M, Kitagawa H, Sugahara K, Rajab A, Höhne W, et al. Loss of chondroitin 6-O-sulfotransferase-1 function results in severe human chondrodysplasia with progressive spinal involvement. Proceedings of the National Academy of Sciences of the United States of America 101:10155-10160 (2004)
5. Duz MB, Topak A. Recurrent c.776T>C mutation in CHST3 with four other novel mutations and a literature review. Clinical dysmorphology 29:167-172 (2020)
6. Albuz B, Çetin GO, Özhan B, Sarikepe B, Anlaş Ö, Öztürk M, et al. A novel nonsense mutation in CHST3 in a Turkish patient with spondyloepiphyseal dysplasia, Omani type. Clinical dysmorphology 29:61-64 (2020)
7. Paganini C, Gramegna Tota C, Superti-Furga A, Rossi A. Skeletal Dysplasias Caused by Sulfation Defects. International journal of molecular sciences 21:(8):2710 (2020)
8. van Roij MH, Mizumoto S, Yamada S, Morgan T, Tan-Sindhunata MB, Meijers-Heijboer H, et al. Spondyloepiphyseal dysplasia, Omani type: further definition of the phenotype. American journal of medical genetics. Part A 146a:2376-2384 (2008)
9. Hermanns P, Unger S, Rossi A, Perez-Aytes A, Cortina H, Bonafé L, et al. Congenital joint dislocations caused by carbohydrate sulfotransferase 3 deficiency in recessive Larsen syndrome and humero-spinal dysostosis. American journal of human genetics 82:1368-1374 (2008)
10. MacNeil JA, Boyd SK. Improved reproducibility of high-resolution peripheral quantitative computed tomography for measurement of bone quality. Medical engineering & physics 30:792-799 (2008)
11. Yu F, Xu Y, Hou Y, Lin Y, Jiajue R, Jiang Y, et al. Age-, Site-, and Sex-Specific Normative Centile Curves for HR-pQCT-Derived Microarchitectural and Bone Strength Parameters in a Chinese Mainland

Population. Journal of bone and mineral research : the official journal of the American Society for Bone and Mineral Research 35:2159-2170 (2020)

12. Burghardt AJ, Buie HR, Laib A, Majumdar S, Boyd SK. Reproducibility of direct quantitative measures of cortical bone microarchitecture of the distal radius and tibia by HR-pQCT. Bone 47:519-528 (2010)
13. Manske SL, Zhu Y, Sandino C, Boyd SK. Human trabecular bone microarchitecture can be assessed independently of density with second generation HR-pQCT. Bone 79:213-221 (2015)
14. Richards S, Aziz N, Bale S, Bick D, Das S, Gastier-Foster J, et al. Standards and guidelines for the interpretation of sequence variants: a joint consensus recommendation of the American College of Medical Genetics and Genomics and the Association for Molecular Pathology. Genetics in medicine : official journal of the American College of Medical Genetics 17:405-424 (2015)
15. Dhawale A, Bajaj S, Chaudhary K, Agarwal T, Garg S, Choudhury H. Posterior Circulation Stroke due to Atlantoaxial Instability in CHST3-Related Skeletal Dysplasia: A Case Report. JBJS case connector 11(2021)
16. Feng L, Li Y, Li Y, Jiang Y, Wang N, Yuan D, et al. Whole exome sequencing detects CHST3 mutation in patient with acute promyelocytic leukemia: A case report. Medicine 97:e12214 (2018)
17. Srivastava P, Pandey H, Agarwal D, Mandal K, Phadke SR. Spondyloepiphyseal dysplasia Omani type: CHST3 mutation spectrum and phenotypes in three Indian families. American journal of medical genetics. Part A 173:163-168 (2017)
18. Ranza E, Huber C, Levin N, Baujat G, Bole-Feysot C, Nitschke P, et al. Chondrodysplasia with multiple dislocations: comprehensive study of a series of 30 cases. Clinical genetics 91:868-880 (2017)
19. Muys J, Blaumeiser B, Jacquemyn Y, Janssens K. Prenatal homozygosity mapping detects a novel mutation in CHST3 in a fetus with skeletal dysplasia and joint dislocations. Clinical case reports 5:440-445 (2017)
20. Waryah AM, Shahzad M, Shaikh H, Sheikh SA, Channa NA, Hufnagel RB, et al. A novel CHST3 allele associated with spondyloepiphyseal dysplasia and hearing loss in Pakistani kindred. Clinical genetics 90:90-95 (2016)
21. Sroka H, Chitayat D. Prenatal diagnosis of autosomal reccessive Larsen syndrome. Prenatal Diagnosis 35:73-74 (2015)
22. Searle C, Jewell R, Kraft J, Stoebe P, Chumas P, Titheradge H, et al. Craniosynostosis: a previously unreported association with CHST3-related skeletal dysplasia (autosomal recessive Larsen syndrome). Clinical dysmorphology 23:12-15 (2014)
23. Tanteles GA, Dixit A, Dhar S, Suri M. Two Somali half-siblings with CHST3-related chondrodysplasia illustrating the phenotypic spectrum and intrafamilial variability. American journal of medical genetics. Part A 161a:2588-2593 (2013)
24. Nizon M, Huber C, De Leonardis F, Merrina R, Forlino A, Fradin M, et al. Further delineation of CANT1 phenotypic spectrum and demonstration of its role in proteoglycan synthesis. Human mutation 33:1261-1266 (2012)

25. Unger S, Lausch E, Rossi A, Mégarbané A, Sillence D, Alcausin M, et al. Phenotypic features of carbohydrate sulfotransferase 3 (CHST3) deficiency in 24 patients: congenital dislocations and vertebral changes as principal diagnostic features. American journal of medical genetics. Part A 152a:2543-2549 (2010)
26. Tuysuz B, Mizumoto S, Sugahara K, Celebi A, Mundlos S, Turkmen S. Omani-type spondyloepiphyseal dysplasia with cardiac involvement caused by a missense mutation in CHST3. Clinical genetics 75:375-383 (2009)
27. Rajab A, Kunze J, Mundlos S. Spondyloepiphyseal dysplasia Omani type: a new recessive type of SED with progressive spinal involvement. American journal of medical genetics. Part A 126a:413-419 (2004)
28. Hall BD. Humero-spinal dysostosis: report of the fourth case with emphasis on generalized skeletal involvement, abnormal craniofacial features, and mitral valve thickening. Journal of pediatric orthopedics. Part B 6:11-14 (1997)
29. Cortina H, Vidal J, Vallcanera A, Alberto C, Muro D, Dominguez F. Humero-spinal dysostosis. Pediatric radiology 8:188-190 (1979)
30. Paganini C, Gramegna Tota C, Superti-Furga A, Rossi A. Skeletal Dysplasias Caused by Sulfation Defects. International journal of molecular sciences 21(2020)
31. Iozzo RV. Matrix proteoglycans: from molecular design to cellular function. Annual review of biochemistry 67:609-652 (1998)
32. Lei J, Yan S, Zhou Y, Wang L, Zhang J, Guo X, et al. Abnormal expression of chondroitin sulfate sulfotransferases in the articular cartilage of pediatric patients with Kashin-Beck disease. Histochemistry and cell biology 153:153-164 (2020)
33. Han J, Li D, Qu C, Wang D, Wang L, Guo X, et al. Altered expression of chondroitin sulfate structure modifying sulfotransferases in the articular cartilage from adult osteoarthritis and Kashin-Beck disease. Osteoarthritis and cartilage 25:1372-1375 (2017)
34. Song YQ, Karasugi T, Cheung KM, Chiba K, Ho DW, Miyake A, et al. Lumbar disc degeneration is linked to a carbohydrate sulfotransferase 3 variant. The Journal of clinical investigation 123:4909-4917 (2013)
35. Fukuta M, Kobayashi Y, Uchimura K, Kimata K, Habuchi O. Molecular cloning and expression of human chondroitin 6-sulfotransferase. Biochimica et biophysica acta 1399:57-61 (1998)
36. Teichtahl AJ, Wluka AE, Wijethilake P, Wang Y, Ghasem-Zadeh A, Cicuttini FM. Wolff's law in action: a mechanism for early knee osteoarthritis. Arthritis research & therapy 17:207 (2015)
37. Gregersen PA, Savarirayan R. Type II Collagen Disorders Overview. In: Adam MP, Ardinger HH, Pagon RA, Wallace SE, Bean LJH, Gripp KW, Mirzaa GM, Amemiya A (eds) GeneReviews(®). University of Washington, Seattle Copyright © 1993-2022, University of Washington, Seattle. GeneReviews is a registered trademark of the University of Washington, Seattle. All rights reserved., Seattle (WA)(1993)
38. Garcia Segarra N, Mittaz L, Campos-Xavier AB, Bartels CF, Tuysuz B, Alanay Y, et al. The diagnostic challenge of progressive pseudorheumatoid dysplasia (PPRD): a review of clinical features,

radiographic features, and WISP3 mutations in 63 affected individuals. American journal of medical genetics. Part C, Seminars in medical genetics 160c:217-229 (2012)

39. Tiller GE. X-Linked Spondyloepiphyseal Dysplasia Tarda. In: Adam MP, Everman DB, Mirzaa GM, Pagon RA, Wallace SE, Bean LJH, Gripp KW, Amemiya A (eds) GeneReviews(®). University of Washington, Seattle Copyright © 1993-2022, University of Washington, Seattle. GeneReviews is a registered trademark of the University of Washington, Seattle. All rights reserved., Seattle (WA)(1993)

Tables

Table 1

Bone geometry, volumetric bone mineral density and bone microarchitecture at radius and tibia between healthy controls and the patient by HR-pQCT.

	Radius			**Tibia**		
	Control	Patient	p	Control	Patient	p
Bone geometry						
Tot.Ar (mm^2)	241.9 ± 45.9	243.7	0.935	624.6 ± 140.1	600.7	0.722
Tb.Ar (mm^2)	192.0 ± 44.1	198.8	0.747	508.9 ± 132.2	536.4	0.666
Ct.Ar (mm^2)	50.9 (49.5 ~ 58.3)	48.5	0.042	120.8 ± 26.3	69.3	0.012
Ct.Pm (mm)	63.2 ± 6.4	67.6	0.196	96.4 ± 10.5	94.3	0.681
Volumetric bone mineral density						
Tot.vBMD (mg HA/cm^3)	301.0 ± 42.6	243.6	0.040	312.2 ± 58.6	191.3	0.010
Tb.vBMD (mg HA/cm^3)	172.8 ± 29.5	128.8	0.029	188.5 ± 45.6	115.6	0.023
Ct.vBMD (mg HA/cm^3)	763.9 ± 40.9	732	0.156	834.0 ± 31.4	802.7	0.090
Bone microarchitecture						
Tb.BV/TV	0.274 ± 0.045	0.156	0.011	0.283 ± 0.061	0.166	0.013
Tb.N (1/mm)	1.578 ± 0.212	1.395	0.127	1.398 ± 0.222	1.457	0.587
Tb.Th (mm)	0.225 ± 0.005	0.218	0.043	0.268 ± 0.029	0.197	0.005
Tb.Sp (mm)	0.597 ± 0.098	0.7	0.079	0.694 ± 0.134	0.677	0.793
Tb.1/N.SD (mm)	0.233 ± 0.058	0.24	0.790	0.305 ± 0.079	0.274	0.425
Ct.Po	0.007 ± 0.003	0.005	0.347	0.019 ± 0.014	0.003	0.072
Ct.Th (mm)	0.963 ± 0.010	0.875	0.121	1.318 (1.225 ~ 1.884)	0.813	0.043
Ct.Po.Dm (mm)	0.170 ± 0.020	0.127	0.008	0.201 ± 0.050	0.141	0.056

Note: Abbreviations: HR-pQCT, high-resolution peripheral quantitative computed tomography; Tot.Ar, total area;Tb.Ar, trabecular area; Ct.Ar, cortical area; vBMD, volumetric bone mineral density; Tot.vBMD, total vBMD; Tb.vBMD, trabecular vBMD; Ct.vBMD, cortical vBMD; Ct.Pm, cortical perimeter; Tb.Th,trabecular thickness; Tb. Sp, trabecular separation;Tb.N, trabecular number;Tb.BV/TV, trabecular bone volume fraction;Tb.1/N.SD, trabecular inhomogeneity of Network; Ct.Po, cortical porosity;Ct.Th, cortical thickness; Ct.Po.Dm, cortical pore diameter.

Table 2

Summary of clinical and radiological characteristics in patients of SED with congenital joint dislocations.

Clinical Characteristics	Proportion (Affected cases/N)	Radiological Characteristics	Proportion (Affected cases/N)
Short stature	100% (72/72)	Abnormal shape of vertebrae	100% (37/37)
Limited joint extension	100% (45/45)	Epiphyseal dysplasia	100% (30/30)
Joint pain	100% (14/14)	Shortening femoral neck	100% (19/19)
Waddling gait	100% (12/12)	Joint enlargement	96.3% (26/27)
Normal intelligence	97.9% (46/47)	Irregular/flat acetabulum	95.0% (19/20)
Joint dislocation/subluxation	97.0% (65/67)	Osteoarthritis	88.5% (23/26)
Rhizomelic shortening	94.9% (37/39)	Delayed bone age	84.2% (16/19)
Thoracic deformities [a]	94.3% (33/35)	Abnormal echocardiography [d]	84.0% (21/25)
Spinal deformities [b]	93.6% (44/47)	Narrowed intervertebral space	81.1% (30/37)
Joint laxity	89.5% (17/19)	Lumbosacral kyphosis	77.8% (21/27)
Genu valgum/varum	88.6% (31/35)	Short phalanges/metacarpals	77.3% (17/22)
Small teeth	81.8% (9/11)	Scoliosis	73.5% (25/34)
Cubitus valgus	81.8% (27/33)	Thoracic kyphosis	67.9% (19/28)
Short neck	79.3% (23/29)	Interpedicular vertebrae widening	57.9% (11/19)
Specific facial features [c]	77.8% (14/18)	Lumbar lordosis	50.0% (9/18)
Restricted activity	72.7% (16/22)	Sacroiliac joint deformity	38.9% (7/18)
Short phalanges	71.4% (25/35)	Vertebral fusion	27.3% (9/33)

Note: a: thoracic deformities include broad chest, barrel-shaped chest and pectus excavatum/carinatum, etc. b: Spinal deformities include thoracic kyphosis, lumbosacral kyphosis, lumbar lordosis and scoliosis, etc. c: specific facial features include sparse or thick eyebrows, hypertolerism, high-arched palate, long philtrum, micrognathia, high anterior hairline and small ears, etc. d: abnormal echocardiography includes mitral and/or tricuspid regurgitation, aortic and/or pulmonary valve stenosis, ventricular septal defect and valve thickening, ect.

Clinical Characteristics	Proportion (Affected cases/N)	Radiological Characteristics	Proportion (Affected cases/N)
Short metacarpals	60.0% (15/25)		
Pes varus	60.0% (33/55)		
Camptodactyly	58.1% (18/31)		
Hearing impairment	42.9% (9/21)		
Megalencephaly and broad forehead	34.8% (8/23)		

Note: a: thoracic deformities include broad chest, barrel-shaped chest and pectus excavatum/carinatum, etc. b: Spinal deformities include thoracic kyphosis, lumbosacral kyphosis, lumbar lordosis and scoliosis, etc. c: specific facial features include sparse or thick eyebrows, hypertolerism, high-arched palate, long philtrum, micrognathia, high anterior hairline and small ears, etc. d: abnormal echocardiography includes mitral and/or tricuspid regurgitation, aortic and/or pulmonary valve stenosis, ventricular septal defect and valve thickening, ect.

Table 3

Differential diagnosis of SED.

SED Type	Pathogenic gene	Inheritance	Onset age	Clinical features	Radiological changes
SEDO	CHST3	AR	Prenatal onset	• Prenatal and postnatal short stature • Joint dislocations at birth or at the first decade • Joint construction, joint pain • Clubfeet, waddling gait • Genu valgum • Some patients had hearing impairment	• X-ray: abnormal vertebrae shape, epiphyseal dysplasia, joint enlargement, scoliosis, delayed or normal bone age, etc. • ECHO: mild cardiac valve dysplasia
SEDC	COL2A1	AD	Perinatal onset	• Severe disproportionate short stature • Short limbs • Special facial features: hypertelorism, flat profile, cleft palate, etc. • Skeletal: short neck, scoliosis, kyphosis, cervical instability, etc. • Some patients suffer joint pain • Ocular abnormalities, hearing loss	• X-ray: delayed epiphyseal ossification, epiphyseal dysplasia, shortening of long bones, flat or ovoid vertebrae, scoliosis, dislocation of hip, etc.

Abbreviations: SED, spondyloepiphyseal dysplasia. SEDO, spondyloepiphyseal dysplasia Omani type, also called spondyloepiphyseal dysplasia with congenital joint dislocations or CHST3-related skeletal dysplasia; SEDC, spondyloepiphyseal dysplasia congenital; SEDT-PA, spondyoepiphyseal dysplasia tarda with progressive arthropathy; SEDT, spondyloepiphyseal dysplasia tarda; CHST3, carbohydrate sulfotransferase 3; COL2A1, type II collagen A1; WISP3, Wnt-inducible signaling pathway protein 3; TRAPPC2, transport protein particle complex 2; AR, autosomal recessive inheritance; AD, autosomal dominant inheritance; XL, X-linked recessive inheritance; ECHO, echocardiography.

SED Type	Pathogenic gene	Inheritance	Onset age	Clinical features	Radiological changes
SEDT-PA	WISP3	AR	3 ~ 6 years old	• Normal at birth • Joint pain, joint stiffness, and joint swelling of all joints, begin with interphalangeal joints, later involvement of large joints • Waddling gait, walking difficulty • Short stature (< 3rd centile) in adolescence • Genu valgum/varum • Weakness • No inflammation	• X-ray: enlarged epiphyses, widened metaphyses, and narrow joint space at hands, enlarged capital femoral epiphyses, acetabular irregularity, platyspondyly, narrowing of intervertebral disc spaces, osteophytic formations, periarticular calcifications, diffuse osteoporosis at the late stage, etc.
SEDT	TRAPPC2	XL	5 ~ 10 years old	• Normal birth length and weight • Short stature, short trunk • Progressive osteoarthritis: joint and back pain, mainly affect hip, knee, and shoulder joints, interphalangeal joints are not affected • Broad chest, genu varum • No extra-skeletal manifestation	• X-ray: normal at early childhood; multiple epiphyseal abnormalities, mild scoliosis, lumbar lordosis, kyphosis, odontoid hypoplasia, flat vertebrae, narrow disc spaces, Coxa vara, short femoral necks

Abbreviations: SED, spondyloepiphyseal dysplasia. SEDO, spondyloepiphyseal dysplasia Omani type, also called spondyloepiphyseal dysplasia with congenital joint dislocations or CHST3-related skeletal dysplasia; SEDC, spondyloepiphyseal dysplasia congenital; SEDT-PA, spondyoepiphyseal dysplasia tarda with progressive arthropathy; SEDT, spondyloepiphyseal dysplasia tarda; CHST3, carbohydrate sulfotransferase 3; COL2A1, type II collagen A1; WISP3, Wnt-inducible signaling pathway protein 3; TRAPPC2, transport protein particle complex 2; AR, autosomal recessive inheritance; AD, autosomal dominant inheritance; XL, X-linked recessive inheritance; ECHO, echocardiography.

Figures

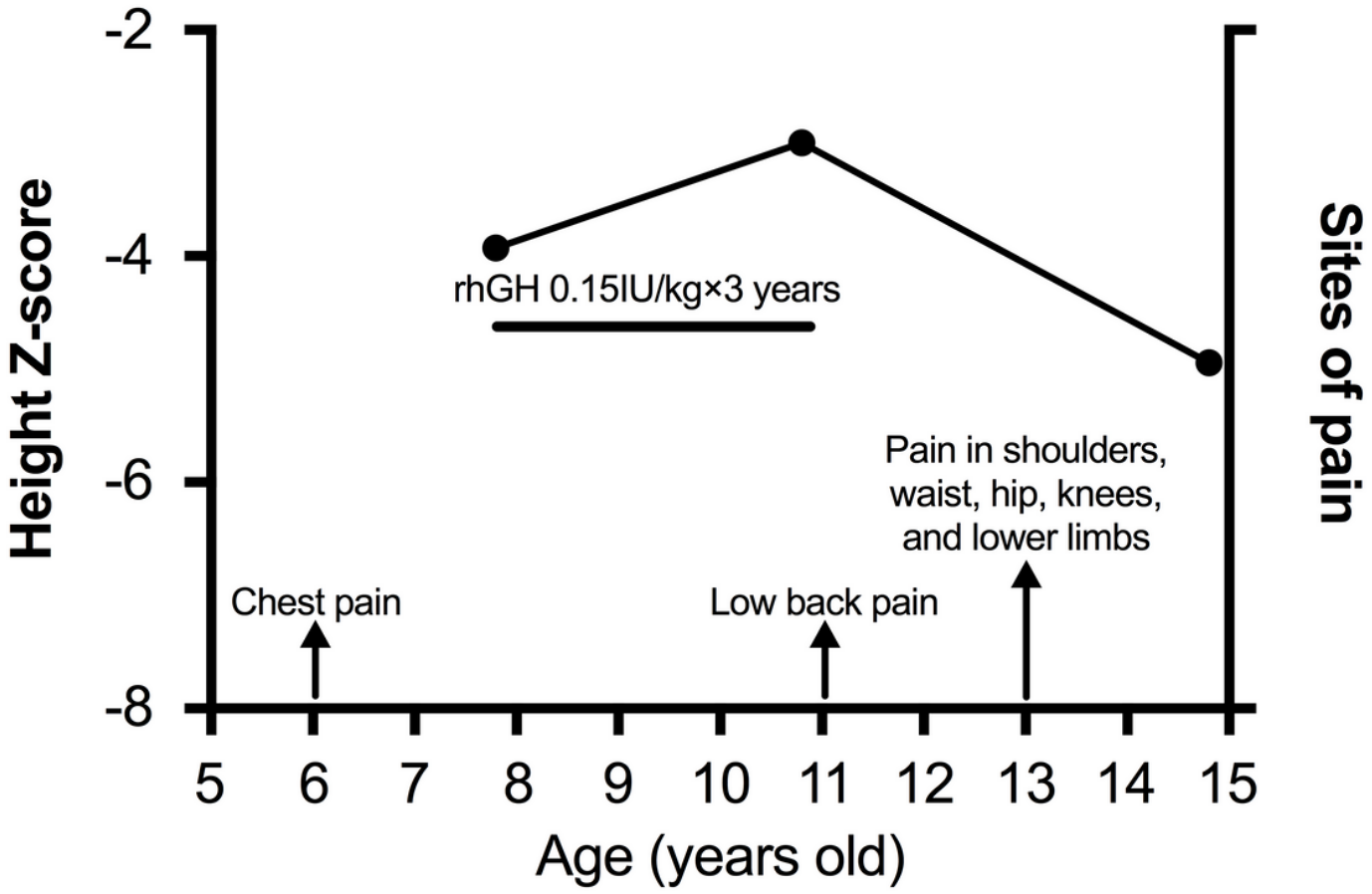

Figure 1

Growth chart and time points of pain onset at different sites of the affected individual. This figure only displays the height Z score and pain information during his childhood and adolescence since his height was not recorded before 7.8 years old and his clinical condition was not severe before 6 years old.

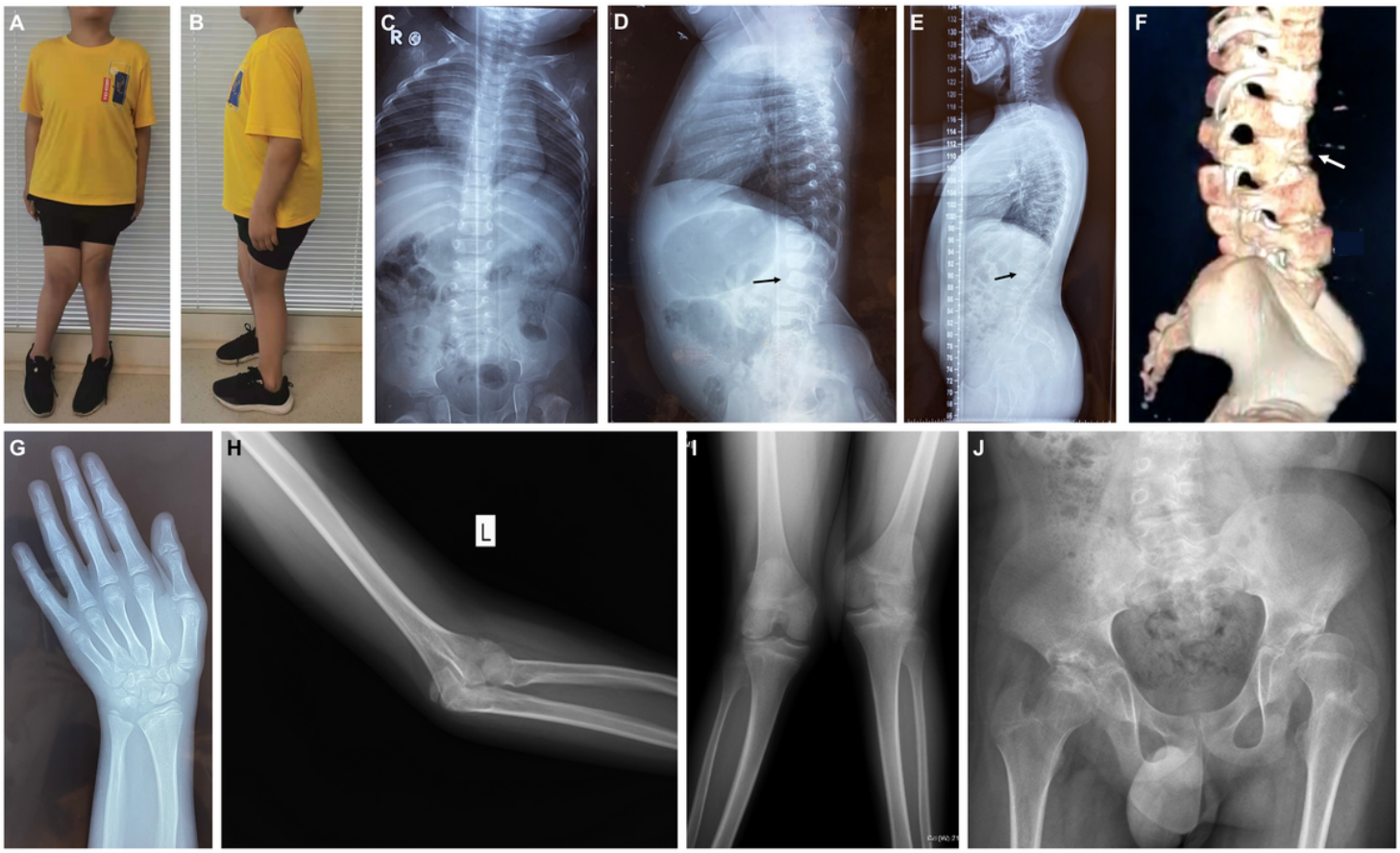

Figure 2

Clinical and radiological characteristics of the proband. (A~B) Clinical images of the proband. (C~D) X-ray of the spine at 1-year-old. The black arrow of Panel D indicates small vertebrae of L2. (E) X-rays of the spine at 14.8 years old, apart from thoracic and sacrum kyphosis and lumbar lordosis, the black arrow shows the compression fracture of L2. (F) The white arrow in the three-dimensional computed tomography also shows the compression fracture of L2. (G) X-ray of the left hand: shortening of the fifth middle phalanx, epiphyseal dysplasia of carpal bones, and structural disorganization of the metaphysis. (H) Enlargement of the left elbow joint. (I) Enlargement of the knee joints, genu valgum, and joint space narrowing of the knee joints. (J) Subluxation of the left hip joint, osteoarthritis of the hip joints and the sacroiliac joints, and scoliosis of the lumbar spine.

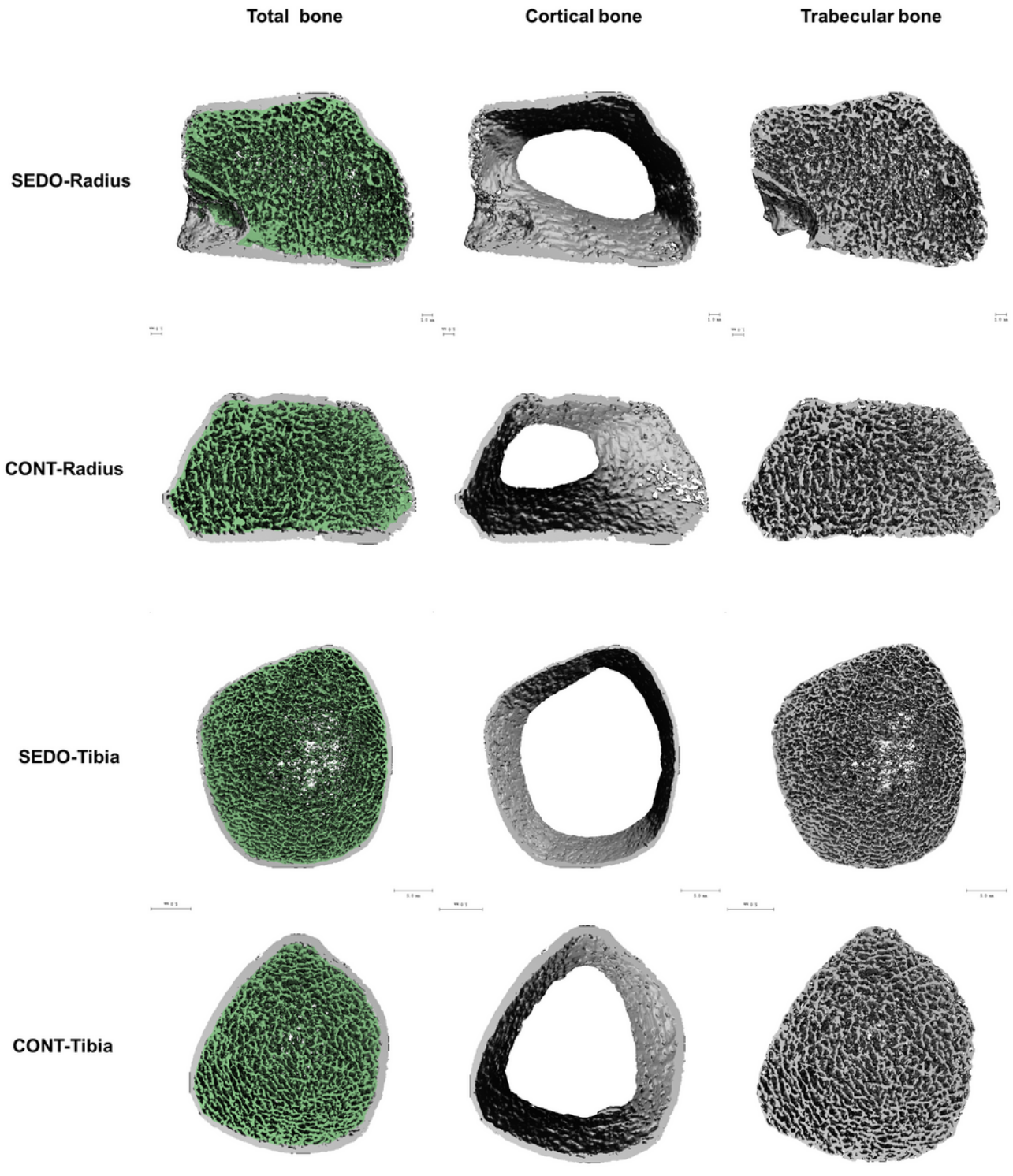

Figure 3

Representative HR-pQCT figures at the distal radius and tibia in the proband with CHST3-related skeletal dysplasia and a 15-year-old healthy boy. SEDO stands for the 14.8-year-old proband with CHST3-related skeletal dysplasia, and CONT represents the healthy boy. The volumetricbone mineral density and trabecular bone microarchitecture of SEDO were inferior tothose of CONT.

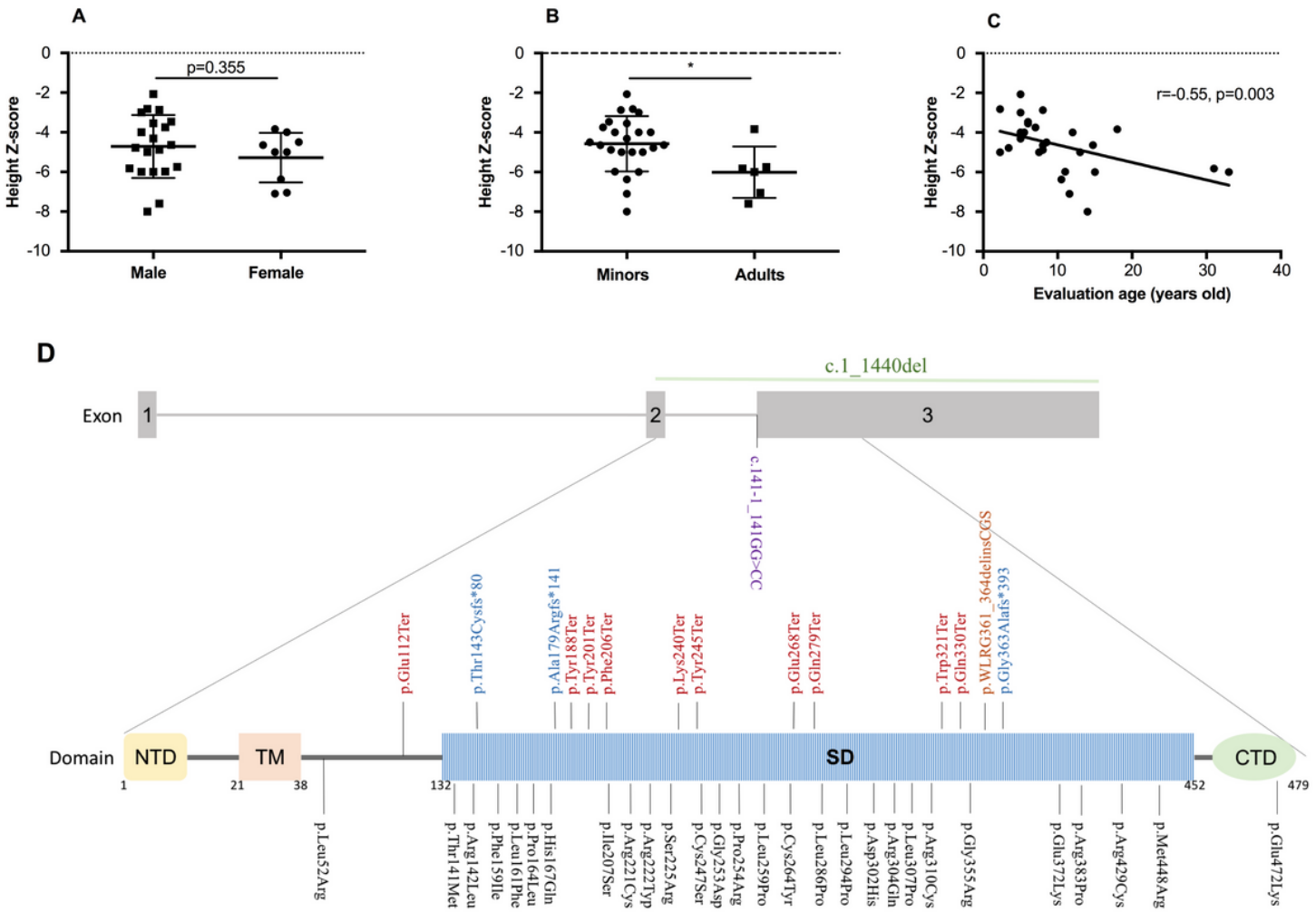

Figure 4

Analysis of height Z scores among patients with CHST3-related skeletal dysplasia and a summary of all reported CHST3 variants. (A) Comparison of the height Z scores between boys and girls. (B) Comparison of the height Z scores of these patients as children and as adults. (C) Bivariate analysis of height Z scores and age at evaluation by Spearman analysis. (D) Summary of all reported *CHST3* variants causing CHST3-related skeletal dysplasia. Variants in black, red, blue, orange, green, and purple represent missense, nonsense, frameshift, indel, deletion, and splicing variants, respectively. Abbreviations: indel, insertion and deletion; *, p<0.05.

Supplementary Files

This is a list of supplementary files associated with this preprint. Click to download.

- SupplementarymaterialsCHST3.docx